Geophysical Research Letters

RESEARCH LETTER
10.1029/2022GL098904

Record Low Antarctic Sea Ice Cover in February 2022

John Turner[1], Caroline Holmes[1], Thomas Caton Harrison[1], Tony Phillips[1], Babula Jena[2], Tylei Reeves-Francois[1], Ryan Fogt[3], Elizabeth R. Thomas[1], and C. C. Bajish[2]

[1]British Antarctic Survey, Natural Environment Research Council, Cambridge, UK, [2]National Centre for Polar and Ocean Research, Goa, India, [3]Ohio University, Athens, OH, USA

Key Points:

- Antarctic sea ice extent dropped to a record low level of 1.92×10^6 km^2 on 25 February 2022
- There were negative sea ice anomalies in all sectors of the Southern Ocean, with the largest in the Ross and Weddell Seas
- Deep storms in October/November 2021 led to low sea ice concentration and a large coastal polynya that accelerated sea ice loss

Supporting Information:

Supporting Information may be found in the online version of this article.

Correspondence to:

J. Turner,
jtu@bas.ac.uk

Citation:

Turner, J., Holmes, C., Caton Harrison, T., Phillips, T., Jena, B., Reeves-Francois, T., et al. (2022). Record low Antarctic sea ice cover in February 2022. *Geophysical Research Letters*, *49*, e2022GL098904. https://doi.org/10.1029/2022GL098904

Received 28 MAR 2022
Accepted 27 MAY 2022

Author Contributions:

Conceptualization: John Turner
Formal analysis: John Turner, Caroline Holmes, Thomas Caton Harrison, Tony Phillips, Babula Jena, Tylei Reeves-Francois, Ryan Fogt, Elizabeth R. Thomas, C. C. Bajish
Methodology: John Turner, Caroline Holmes, Babula Jena, Tylei Reeves-Francois
Software: John Turner, Caroline Holmes, Thomas Caton Harrison, Tony Phillips, Babula Jena, C. C. Bajish
Supervision: John Turner
Writing – original draft: John Turner
Writing – review & editing: Caroline Holmes, Thomas Caton Harrison, Tony Phillips, Babula Jena, Ryan Fogt, Elizabeth R. Thomas

Abstract On 25 February 2022 Antarctic sea ice extent dropped to a satellite-era record low level of 1.92×10^6 km^2, 0.92×10^6 km^2 below the long-term mean. The area of sea ice was also at a record low level of 1.24×10^6 km^2. Although no individual sector was at a record low, at the minimum there were negative sea ice anomalies in all sectors of the Southern Ocean, with the largest in the Ross (contributing 46%) and Weddell Seas (26%). The Amundsen Sea Low had a record low depth in October/November 2021, with a series of very deep depressions giving strong offshore winds. These accelerated ice loss during the melt season, creating a 1.00×10^6 km^2 coastal polynya in the Ross Sea. In the northern Weddell Sea, westerly winds of record strength led to ice export from the region.

Plain Language Summary Sea ice is a critical part of the Antarctic climate system that is an important breeding habitat for seals and other marine biota, as well as playing an important part in the global ocean circulation. Unlike the Arctic, where sea ice extent has decreased over recent decades, sea ice around the Antarctic actually increased in extent for a large part of the record starting in the late 1970s. However, on 25 February 2022 the extent dropped to a record low level of 1.924 million square kilometers, 1 million square kilometers below the long-term average. The origins of the sea ice loss can be traced back to extremely deep storms in the Ross Sea in October and November 2021, and the very strong southerly winds that the storms had on their western flank. These moved sea ice away from the Antarctic coast, exposing the ocean and allowing solar heating to warm the ocean and give further sea ice melt. An additional factor was the very strong westerly winds north of the Weddell Sea that moved sea ice out of this basin and toward the east.

1. Introduction

Antarctic sea ice extent (SIE) has displayed a complex pattern of change over the period for which we have reliable data from passive microwave satellite instruments starting in the late 1970s. Until the mid-1990s there was no significant trend in the annual mean total Antarctic SIE or the extent at the annual minimum (Figure 1a). However, this was followed by an upward trend in both measures, which was accompanied by an increase in the inter-annual variability (Fogt et al., 2022, Figure 1). The overall increase in SIE between the mid-1990s and 2014 masked large regional variations, such as the increase in the Ross Sea and decrease in the Amundsen-Bellingshausen Seas (ABS) (Turner et al., 2015), which was consistent with a deepening of the Amundsen Sea Low (ASL) (Raphael et al., 2015). A number of studies have examined the sea ice increase and suggested it was linked to a range of high latitude and tropical forcing factors (Holland et al., 2017; Meehl et al., 2016; Stammerjohn et al., 2008). It seems likely that more than one factor was responsible.

Following the record maximum annual mean SIE in 2014 the extent dropped dramatically, with record or near-record low extent in 2017 in the annual daily maximum and minimum, and also the annual mean extent (Figure 1a). The most anomalous decrease took place during spring (September–November) 2016, and was largest in the Weddell and Ross Seas.

After 2017 there was a modest recovery in the annual mean SIE, although the values for 2018–2021 were much lower than for the peak in 2014. From mid-October 2021 the sea ice began an early retreat (Figure S1a in Supporting Information S1), reaching a record low SIE of 1.92×10^6 km^2 on 25 February 2022, which was 0.92×10^6 km^2 below the long-term mean. The area of sea ice was also at a record low level of 1.24×10^6 km^2.

The SIE over the Southern Ocean is influenced by the major modes of climate variability, including the Southern Annular Mode (SAM) (Lefebvre et al., 2004) and the El Niño-Southern Oscillation (Turner, 2004). Anomalously strong westerly winds when the SAM is in its positive phase can affect the speed of the Weddell gyre (Vernet

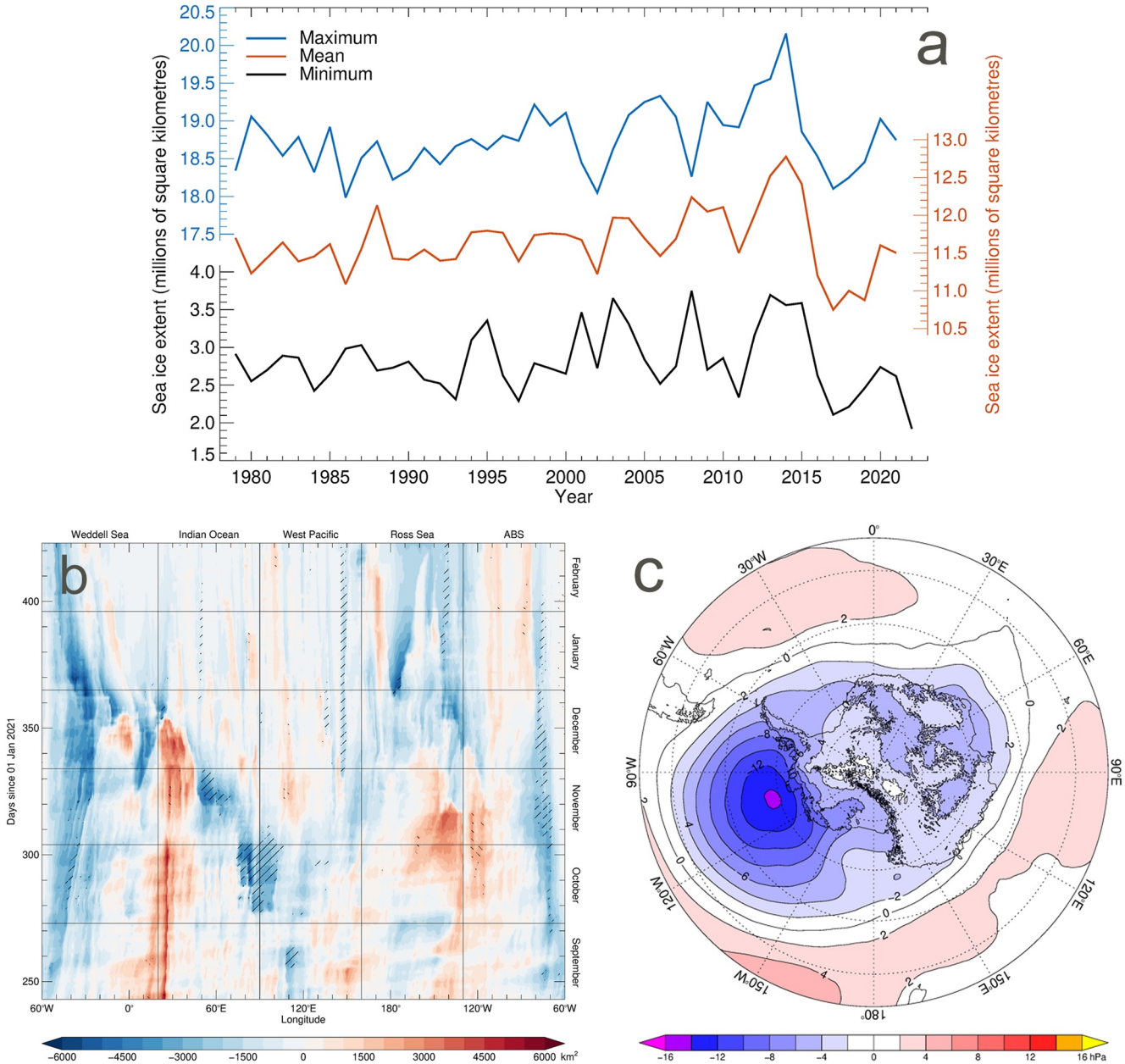

Figure 1. (a) The minimum daily sea ice extent (SIE) (10^6 km^2) for the Southern Ocean along with the daily maximum and annual mean for 1979–2022. (b) The SIE anomalies for September 2021–February 2022 by 0.2° longitude bands. The hatching indicates where the ice extent anomalies in 2021-22 were extreme—that is, where the SIE in 2021-22 lay outside the range for that longitude band and day across the 30 years 1991-92–2020-21. Hatching from top-right to bottom-left on blue regions indicates extreme negative anomalies; hatching from top-left to bottom-right on red regions indicates extreme positive anomalies. (c) The ERA5 mean sea level pressure anomaly in spring 2021.

et al., 2019) and lead to more ice export from the Weddell basin. When the tropical Pacific Ocean is in a La Niña state the ASL is deeper (Li et al., 2021) with anomalously strong southerly winds north of the Ross Ice Shelf and more equatorward sea ice transport. The ASL is deeper when the SAM index is positive (Fogt et al., 2012), so the low is particularly deep during periods of positive SAM/La Niña (Fogt & Bromwich, 2006).

Large scale atmospheric circulation anomalies are important in modulating SIE concurrently (Raphael & Hobbs, 2014) and at several months lead-lag (Holland et al., 2018). However, the evolution of the melt season and eventual minimum also depends greatly on local atmospheric extremes operating on daily timescales.

Here we examine the development of the February 2022 record low SIE using daily satellite-derived SIE data and high-resolution operational surface analyses. In Section 2 we describe the data used. Section 3 examines the climatological factors that drive interannual variability in the annual minimum SIE. In Section 4 we consider the evolution of the SIE anomalies around the Southern Ocean from the start of September 2021 to the minimum in February 2022 and relate these to the atmospheric circulation anomalies. Section 5 summarizes the event and discusses the 2022 minimum in relation to estimates of pre-satellite era sea ice variability.

2. Data and Methods

Sea ice variability and change were examined using daily (5-day trailing mean), monthly, seasonal and annual sea ice data obtained from the U.S. National Snow and Ice Data Center Sea Ice Index (Fetterer et al., 2017 updated daily). A number of algorithms have been employed to convert the satellite measurements into sea ice concentration (SIC). The Fetterer et al. (2017 updated daily) data use the NASA Team algorithm 1.1 SIC values (Cavalieri et al., 1996 updated yearly), as data derived using this algorithm are available as a consistent time series from late 1978 to May 2021. For more recent occasions we use the NASA Team Near-Real-Time data (Meier et al., 2021). Sea ice area (SIA) was computed as the mean SIC within a region multiplied by the size of the area, with SIE calculated as the total area of all satellite pixels where the SIC equaled or exceeded 15%. SIE is a measure of the region covered by ice that has a significant fraction and is relatively robust to different remote sensing algorithms. SIA is more sensitive to small changes in SIC, such as occur at the start of the melt season, but it varies more between products. As well as the total ice cover over the Southern Ocean, we also considered the SIE in five sectors around the continent that have been used in many earlier studies. These are the Ross Sea (160°E–130°W), the ABS (130°W–60°W), the Weddell Sea (60°W–20°E), the Indian Ocean (20°E–90°E) and the West Pacific sector (90°E–160°E). Ice drift motion data were obtained from the Eumetsat Ocean and Sea Ice Satellite Applications Facility (https://osi-saf.eumetsat.int/products/osi-405-c).

Anomalies were computed as differences from the 30-year base period starting 1 September 1989. Daily anomalies were taken as the difference from the mean 30-year SIE on that day of the year.

Atmospheric circulation was considered using the surface fields for 1979–2020 from the ERA5 reanalysis produced by the European Centre for Medium-range Weather Forecasts (ECMWF) (Hersbach et al., 2020). These have a horizontal grid spacing of approximately 31 km and data are available every hour. For 2021 and 2022 we used the ECMWF operational fields, which have a horizontal grid spacing of approximately 8 km.

3. Factors Controlling the Amount of Sea Ice at the Annual Minimum

The long-term average of annual sea ice maxima of 18.68×10^6 km^2 occurs on 24 September, with a decline until an average minimum of 2.90×10^6 km^2 on 19 February. By this date the largest proportion, 45% (1.33×10^6 km^2, standard deviation (sd) 0.31×10^6 km^2) of ice that has survived the summer melt is in the Weddell Sea sector, but with 19% (0.56×10^6 km^2, sd 0.26×10^6 km^2) in the Ross Sea. The remaining ice is located in the ABS (14%, 0.40×10^6 km^2, sd 0.12×10^6 km^2), the West Pacific Ocean (14%, 0.41×10^6 km^2, sd 0.12×10^6 km^2) and Indian Ocean (8%, 0.22×10^6 km^2, sd 0.09×10^6 km^2). The total Southern Ocean SIE at the minimum is therefore strongly influenced by the amount of sea ice remaining in the Ross and Weddell Seas (Figure S2 in Supporting Information S1).

To investigate the atmospheric conditions that influence sea ice at the annual minimum we examine the composite mean sea level pressure (MSLP) difference of the lower – upper quartile of sea ice minimum extent years (Figure 2). The focus is particularly on October and November as these are the months when the most statistically significant differences are found in MSLP. In addition, the importance of this period has been highlighted in earlier work considering sea ice variability (Holland et al., 2017, 2018).

The signal for the Ross Sea (Figure 2, left column) shows a significantly deep ASL in October and November, with a positive MSLP anomaly to the west in November, ahead of a low SIE minimum. This is consistent with anomalously southerly winds that favor open water near the coast, along with thin, low SIC that can increase the rate of ice loss through to February due to the ice-albedo feedback.

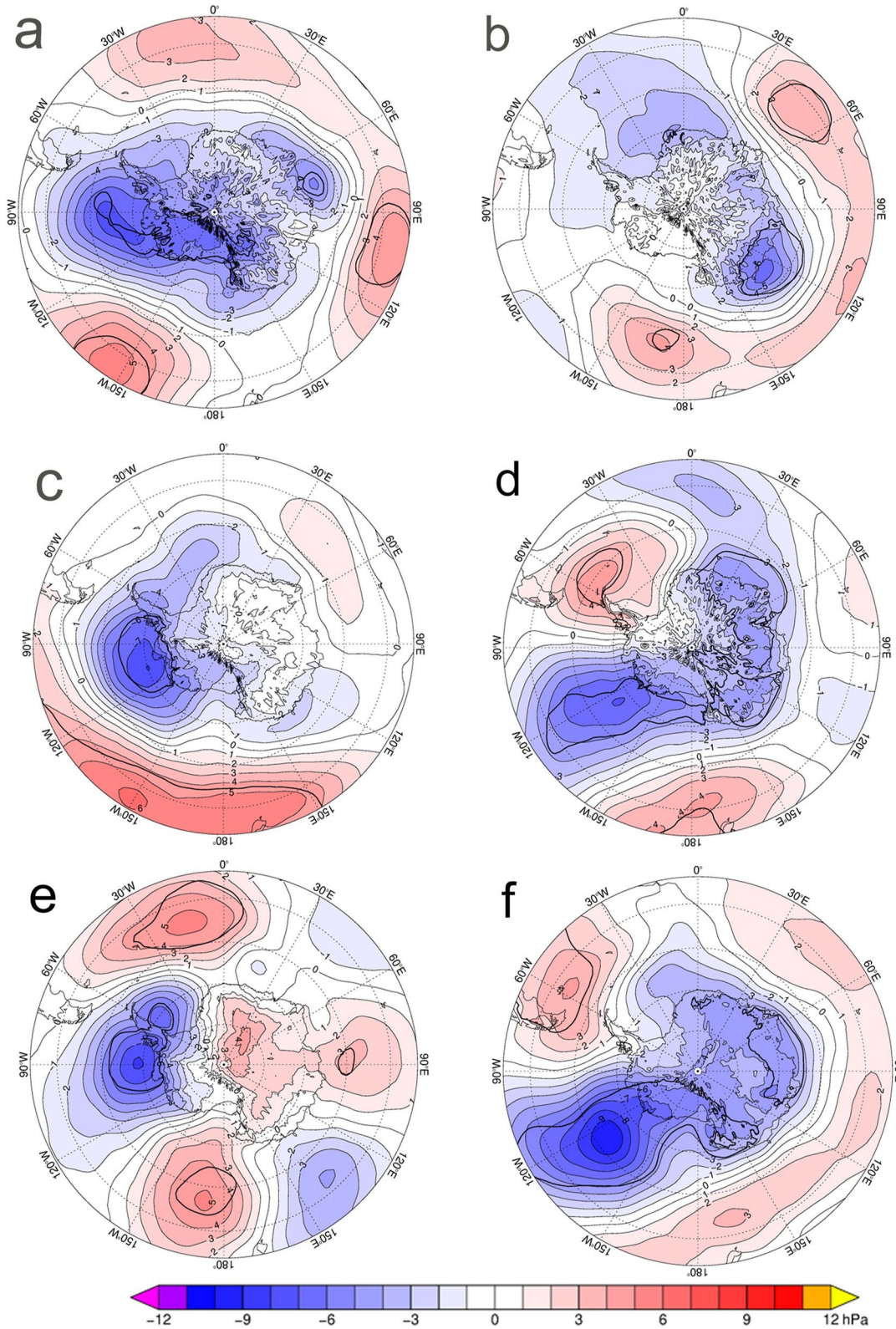

Figure 2. The composite ERA5 mean sea level pressure differences of the lower – upper quartile of sea ice minimum extent years. Differences are for September (top), October (middle) and November (bottom) and the Ross Sea (left) and the Weddell Sea (right). The bold lines indicate areas where the difference is significant at $p < 0.05$.

The MSLP signature for the Weddell Sea SIE (Figure 2, right column) also indicates the importance of a deep ASL for negative SIE anomalies. However, in addition, low MSLP over the continent and high pressure in lower latitudes (especially over the South Atlantic) will lead to stronger west to northwesterly winds across the Weddell Sea and favor ice export toward the east in the lead-up to the sea ice minima. These MSLP anomalies are characteristic of the positive phase of the SAM, suggesting less sea ice at the minimum following a positive SAM in the previous October and November.

These results add to evidence that the depth of the ASL is important in spring in order to precondition the sea ice ahead of the annual minimum. However, the creation of SIE anomalies is episodic and often linked to deep polar cyclones and localized wind extremes (e.g., Jena, Bajish, Turner, Ravichandran, Kshitija, et al., 2022; Jena, Bajish, Turner, Ravichandran, Kumar, & Kshitija, 2022; Kohout et al., 2014; Vichi et al., 2019), with their subsequent maintenance depending on absorption of solar radiation and the nonlinear ice-albedo feedback.

4. The 2021/2022 Sea Ice Melt Season

4.1. Hemispheric and Regional SIE Evolution

In 2021 the total Antarctic SIE had an early maximum of 18.80×10^6 km^2 on 30 August, when the ice was more extensive than the long-term mean maximum, with two notable positive anomalies: east of the Greenwich Meridian (near 30°E) and in the Ross Sea sector (150°–120°W, Figure 1b). The positive anomaly near 30°E persisted until mid-December, while that in the Ross Sea stopped abruptly in mid-November. The negative SIC anomaly close to 50°W over the western Weddell Sea and immediately to the east of the Antarctic Peninsula was a persistent feature over September 2021–February 2022 (Figure 1b). In the first 3 months after the sea ice maximum, when the ice edge was north of the Antarctic Peninsula (Figure S3 in Supporting Information S1), the negative anomaly moved toward the east in the climatological westerly flow (Figure 1b), reaching a maximum in December and early January 2022. After that time, it declined slightly and shifted back toward 50°W. During January and February, the greatest shift to a negative SIE anomaly took place in the Ross Sea sector and especially between 180°W and 120°W. In the ABS there were both positive and negative anomalies.

At the sea ice minimum on 25 February 2022 all five sectors around the continent had negative SIE anomalies, with the largest contribution (46.3%, i.e., the anomaly contributions on the day of minimum) coming from the Ross Sea sector, where the anomaly was -0.46×10^6 km^2. A further 26.1% of the anomaly (-0.26×10^6 km^2) came from the Weddell Sea, with the remaining contributions being 14.6% (-0.14×10^6 km^2) from the West Pacific, 10.6% (-0.10×10^6 km^2) from the Indian Ocean sector and 2.4% (-0.02×10^6 km^2) in the ABS. Although the total Southern Ocean SIE was at a record minimum in February 2022, none of the five sectors around the continent had a record low SIE. The Ross Sea minimum in 2022 was 0.12×10^6 km^2, the second lowest annual extent in the record (the record low SIE was 0.06×10^6 km^2 set on 18 February 2017). The minimum extent in the Weddell Sea in 2022 was 1.09×10^6 km^2, which was the 12th lowest SIE, with the lowest being 0.78×10^6 km^2 on 20 February 1999. The West Pacific, Indian and ABS sectors were respectively the eighth, eighth and fourteenth lowest in the 43-year record. We therefore focus particularly on the Ross and Weddell sectors as they made the greatest contribution to the February 2022 negative SIE anomaly.

The February 2022 total Southern Ocean mean SIE of 2.15×10^6 km^2 was the lowest in the monthly mean SIE record, although none of the previous months since the September 2021 sea ice maximum had a record low value. However, the total SIA was at a record low level from December 2021 to February 2022. Regionally, no sector had its lowest monthly mean SIE in February 2022. The Ross Sea, which contributed the most to the overall negative sea ice anomaly on 25 February 2022, had only its fourth lowest February SIA.

4.2. The Ross Sea

Between September and December 2021, the ASL was anomalously deep, with a hemisphere-wide negative MSLP anomaly in most months (Figure S4 in Supporting Information S1). During spring 2021 the mean MSLP anomaly across 60°–75°S, 50°–180°W, an area previously used to consider ASL variability (Turner et al., 2013), was the lowest from ERA5 data, with the anomaly having a central value below −14 hPa (Figure 1c). The deep ASL led to enhanced southerly flow, with spring mean 10 m southerly wind anomalies of >3 ms^{-1} over approximately 100°W–160°W (box 1 in Figure 3a). The wind speed anomaly was largest in October when the deep

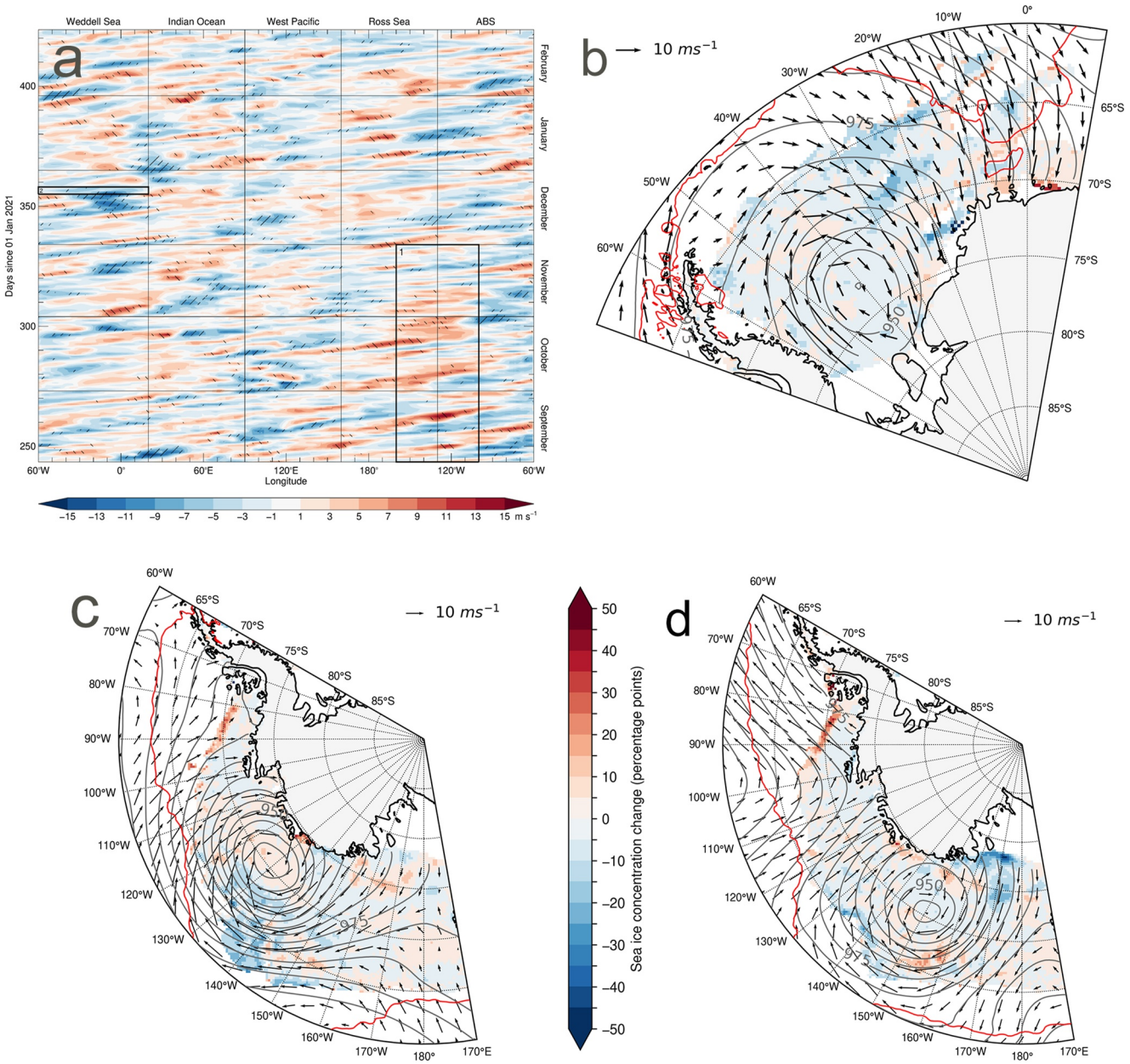

Figure 3. (a) The daily mean 10 m meridional wind anomaly for September 2021–February 2022 by 0.25° longitude bands. Box 1 outlines Spring (September–November), 100°W–160°W. Box 2 outlines 22–24 December, 60°W–20°E. The change in NSIDC sea ice concentration relative to the previous day (shaded background) for (b) the Weddell Sea on the 21 December 2021 and (c and d) the Ross Sea on the 14 November and 21 November respectively. Day-mean mean sea level pressure (MSLP) is overlain in gray contours at 5 hPa intervals (950 and 975 hPa levels labeled) as well as the day-mean 0°C 2 m temperature isotherm (red line) and 10 m wind vectors. MSLP, temperature and winds are from ERA5.

ASL was accompanied by anomalous high pressure between 180° and 90°E (Figure S4b in Supporting Information S1). This led to strong northward transport of sea ice across the Southern Ross Sea (Figure S5 in Supporting Information S1).

As a result of the intense southerlies, by mid-October a band of low-concentration sea ice was present anomalously far north in the Ross Sea (Figure 4b). November 2021 then brought a rapid decline in the Ross Sea SIE, with a particularly large drop occurring over 13–16 November when the ice retreated by $>0.2 \times 10^6$ km^2 (Figure S1b in Supporting Information S1). This was the largest November 3-day retreat in the record and occurred during the passage of an extremely deep depression along the West Antarctic coast on 14 November (Figure 3c).

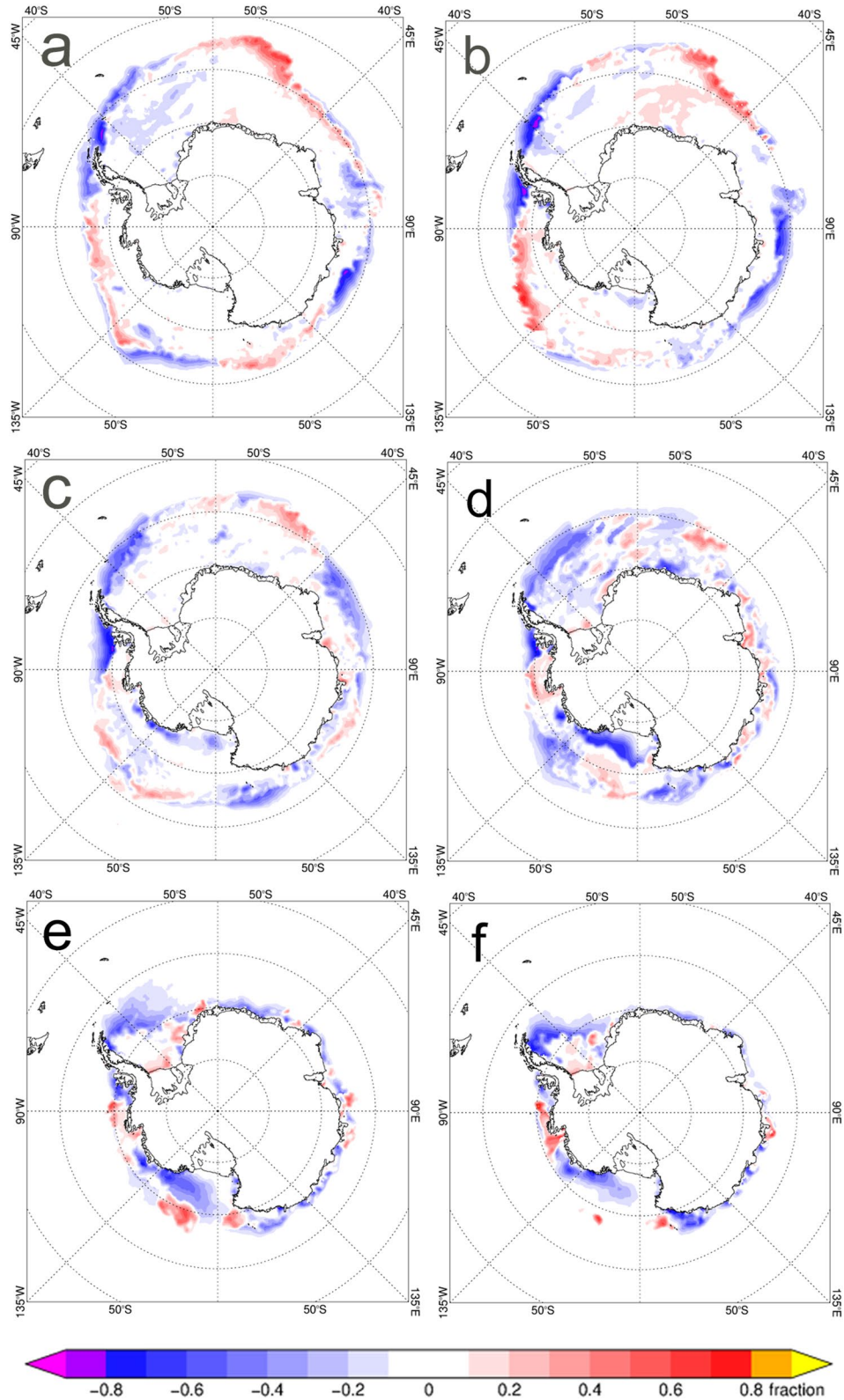

Figure 4. The sea ice concentration anomalies for (a) 15 September 2021, (b) 15 October 2021, (c) 15 November 2021, (d) 15 December 2021, (e) 15 January 2022, and (f) 15 February 2022.

Most of the sea ice loss on this date occurred in the northern band of low-concentration sea ice (north of 70°S), with little indication of sea ice increases nearby on the day (Figure 3c) or on subsequent days. This ice loss was collocated with the region of peak westerly winds (reaching 30 m s^{-1}) to the west and north of the storm center, suggesting sea ice divergence due to northwards Ekman transport in and around the marginal ice zone may have had an important role (e.g., Figure 11 in Eayrs et al., 2019) as well as mechanical breakup due to ocean waves. This ice loss event marked the switch from positive to negative SIE anomalies in the Ross Sea sector (Figure 1b).

Further south, a polynya was already present off the Ross Ice shelf in mid-November (Figure S3c in Supporting Information S1) but its growth was accelerated by a further storm on 21 November which featured a southerly flow positioned directly over the ice shelf edge (Figure 3d).

In December, MSLP remained anomalously low between 135°W and 180°W (Figure S4d in Supporting Information S1), and anomalously strong southerlies persisted off the Ross Ice Shelf. Four more rapid sea ice retreat episodes were spread through the month, with 3-day ice declines in each of about 0.1–0.2 × 10^6 km^2 (Figure S1b in Supporting Information S1). The largest of these was associated with a deep storm on 6 December whose trajectory and peak winds resembled a weaker version of the 14 November storm, whereas that of 9–10 December was more reminiscent of the Ross Ice Shelf southerly flow event of 21 November (Figure 3d). By the middle of the month, large negative SIC anomalies were present between 135°W and 180°W south of 70°S, indicating the polynya was anomalously extensive (Figure S3d in Supporting Information S1).

The passage of the storms in November and December led to favorable conditions for upwelling of sub-surface warm high-salinity water to the mixed layer (Figures S6a–S6c in Supporting Information S1). In parallel, there were anomalous gains of heat of up to ∼100 Wm^{-2} at the ocean surface that contributed to the observed temperature anomaly of up to ∼0.8°C. This was as large as any mixed layer temperature anomaly at this location in the ORAS5 reanalysis data set, and matched only by the temperature anomaly observed in 2017 (Figures S6a and S6b in Supporting Information S1).

The lowest annual minimum SIE in the Ross Sea occurred on 18 February 2017 when the ice covered 0.06 × 10^6 km^2. The trajectory of sea ice loss was rather different from that of 2021/22 (Figure S1b in Supporting Information S1). In 2017 a more rapid decrease in SIE occurred in the second half of January, and by the start of February the differences in SIC between 2017 and 2022 were confined to a small area near the coast just west of 180°. Here the sea ice decreased more until the minimum in 2017 than in 2022, indicating that melt in the few weeks and days ahead of the annual minimum, as well as conditions late in the previous year, can be critical in dictating whether a record low SIE occurs.

4.3. The Weddell Sea

During December 2021 there was anomalously low MSLP over the continent and high MSLP anomalies to the north (Figure S4d in Supporting Information S1), and the mean monthly zonal wind speed north of the Weddell Sea (55°–65°S, 60°–20°W) was 8.1 ms^{-1}, the largest December mean on record. The deep ASL also resulted in a slightly more northwesterly flow into the Weddell Sea, which brought warm airmasses into the region, with the ECMWF operational analyses having temperatures above 0°C as far south as 72°S. These conditions led to negative SIC anomalies along the northern ice edge of the sea ice from the Antarctic Peninsula to the Greenwich Meridian (Figure 4d) as there was anomalously large sea ice advection toward the east (Figure 1b). The negative SIC anomalies along the northern limit of the sea ice were present from September to February, with positive anomalies off the Ronne Ice Shelf and Coates Land as a result of enhanced north to northwesterly flow for much of the melt season. A positive MSLP anomaly in the central Weddell Sea in January with greater flow from the north to the east of the Antarctic Peninsula also contributed to the extensive ice off the Ronne Ice Shelf by the day of ice minimum.

The anomalously strong westerly winds helped to maintain the coastal polynya along the eastern side of the Antarctic Peninsula, which grew steadily from mid-November (Figure 4). An enhanced westerly flow across the peninsula also leads to warming of the air by the foehn effect as it passes over this 2 km high orographic barrier. The warm air arriving over the northwest Weddell Sea would also lead to melting of the sea ice as well as maintaining the polynya.

As in the Ross Sea, the Weddell Sea experienced a number of rapid decreases in SIE over several days (Figure S1c in Supporting Information S1). The most significant of these occurred over 22–24 December, when the sea ice retreated by ~0.4×10^6 km^2 (the meridional wind anomaly is indicated in box 2 on Figure 3a). This was associated with a deep storm that moved into the central Weddell Sea (Figure 3b), advecting warm air down the coast of Coates Land. The strong MSLP gradient to the northeast of the low centre also led to export of sea ice toward the east and out of the sector.

5. Summary and Discussion

The total Antarctic SIE reached a record low level in 2022 because of the presence of negative sea ice anomalies in all sectors of the continent, but particularly in the Ross Sea. In October/November 2021, the ASL had a record low depth, which led to southerly winds of record strength off the continent. The role of the ASL in this season's sea ice evolution was consistent with previous work, which showed that a deeper ASL leads to greater ice transport away from the Ross Ice Shelf and coastal areas to the east, and the generation of new, thin ice over the southern Ross Sea (Comiso et al., 2011). In late 2021 the strong offshore flow resulted in an anomalously northern sea ice edge which was then rapidly eroded by the passage of a series of intense polar cyclones, and also favored the establishment of a large coastal polynya by early December, which was associated with an unusually high-salinity (dense) water mass and upper ocean warming of up to ~0.8°C. Open water then allowed the absorption of solar radiation at the time of its maximum intensity in December, which aided the further loss of sea ice through the ice-albedo feedback.

A further factor that led to the record SIE in February was the positive phase of the SAM in the previous spring. As noted earlier, a positive SAM combined with La Niña conditions favors a deep ASL. Yet such conditions have occurred before without Antarctic sea ice reaching such a low level. Examination of the SAM index and Niño 3.4 temperature anomaly in spring (Figure S7 in Supporting Information S1) shows that low February SIE in the Ross Sea has occurred in some years without positive SAM/La Niña conditions the previous spring. This suggests the configuration of regional circulation anomalies, including the impacts of individual storms in late spring and early summer are also important in establishing negative sea ice anomalies in the Ross Sea. Once established, these negative SIC anomalies can then expand rapidly throughout the summer when solar radiation is at a maximum ahead of the SIE in the following February.

The positive SAM in spring 2021 also contributed to the record strength of the westerly winds north of the Weddell Sea that aided the export of sea ice to the east and the formation of a polynya east of the Antarctic Peninsula. Although the SIE in the Weddell Sea was only the 12th lowest in the record, it was the simultaneous low SIEs in both the Ross and Weddell sectors that was important in establishing the record low SIE for the whole Southern Ocean.

Sea ice reconstructions, based on principal component regression of Southern Hemisphere midlatitude temperature and pressure observations, suggest that the 2022 minimum was one of the lowest of the past 100 years (Fogt et al., 2022). This is supported by sea ice reconstructions from ice cores (Thomas et al., 2019), and data assimilation approaches (Fogt et al., 2022). Most reconstructions suggest that total Antarctic SIE has been declining during the 20th century (Fogt et al., 2022), and it is only after the 1980s that a positive trend is observed. On a regional scale, SIE in the Bellingshausen Sea (Abram et al., 2010) and Indian Ocean (Curran et al., 2003) has been steadily declining during the 20th century. While in the Ross Sea, significant sea-ice expansion has occurred since the ~1940s (Dalaiden et al., 2021), with SIE during the late 20th century higher than at any time during the past ~300 years (Thomas & Abram, 2016). Thus, SIE as low as the 2022 anomaly may have occurred in the Ross Sea sector during the early 20th century. However, unlike the 2022 event, this would have been accompanied by comparably higher SIE in the Bellingshausen and Weddell Seas (Dalaiden et al., 2021; Fogt et al., 2022; Thomas et al., 2019). The abrupt shift to negative anomalies in all sectors appears unusual in the context of the past few centuries (Thomas et al., 2019; Yang et al., 2021), but could arguably be seen as a return to the negative SIE conditions apparent during the early 20th century.

Because of the large and unexpected variability in the Antarctic SIE since the record started in 1978 it is impossible at this time to say whether the decrease in SIE that has been seen over the last several years will continue. Further, the lack of accurate sea ice volume estimates means we cannot say whether there has been an overall thinning of sea ice over this period, which would be an early indicator of longer-term loss. Climate models predict

that there will be a decrease in SIE over the coming decades, but these models failed to anticipate the increase in SIE that took place up to 2016. However, further investigation of the changes that have taken place since the late 1970s through observational studies and model experiments will hopefully shed light on the mechanisms responsible for past changes and help improve our ability to predict future conditions.

Data Availability Statement

The ERA5 hourly fields are available from the Copernicus Climate Data Store, https://doi.org/10.24381/cds.bd0915c6. Ice drift motion data are available from the Eumetsat Ocean and Sea Ice Satellite Applications Facility (https://osi-saf.eumetsat.int/products/osi-405-c). Sea ice extent and area data are available from the U.S. National Snow and Ice Data Center via https://nsidc.org/arcticseaicenews/sea-ice-tools/. Specific files used include S_Sea_Ice_Index_Regional_Daily_Data_G02135_v3.0 and S_Sea_Ice_Index_Regional_Monthly_Data_G02135_v3.0 for the regional daily and monthly data respectively. The Antarctic-wide monthly and annual data was obtained from Sea_Ice_Index_Monthly_Data_by_Year_G02135_v3.0.

Acknowledgments
This work forms part of the Polar Science for Planet Earth program of the British Antarctic Survey. C. Holmes and J. Turner received funding under Natural Environment Research Council large grant DEFIANT NE/W004747/1. R. Fogt acknowledges support from National Science Foundation Grant No. PLR-1744998. We are grateful to NSIDC for the provision of the sea ice data and to European Center for Medium-range Weather Forecasts (ECMWF) for the ERA5 fields. This work contains modified Copernicus Climate Change Service information 2021. Neither the European Commission nor ECMWF is responsible for any use that may be made of the Copernicus information or data it contains. The data set Hersbach et al. (2018) was downloaded from the Copernicus Climate Change Service (C3S) Climate Data Store.

References

Abram, N. J., Thomas, E. R., McConnell, J. R., Mulvaney, R., Bracegirdle, T. J., Sime, L. C., & Aristarain, A. J. (2010). Ice core evidence for a 20th century decline of sea ice in the Bellingshausen Sea, Antarctica. *Journal of Geophysical Research: Atmospheres*, *115*(D23), D23101. https://doi.org/10.1029/2010JD014644

Cavalieri, D. J., Parkinson, C. L., Gloersen, P., & Zwally, H. J. (1996). *Sea Ice concentrations from Nimbus-7 SMMR and DMSP SSM/I-SSMIS passive microwave data*. Version 1, NASA National Snow and Ice Data Center Distributed Active Archive Center. https://doi.org/10.5067/8GQ8LZQVL0VL

Comiso, J. C., Kwok, R., Martin, S., & Gordon, A. L. (2011). Variability and trends in sea ice extent and ice production in the Ross Sea. *Journal of Geophysical Research*, *116*(C4), C04021. https://doi.org/10.1029/2010JC006391

Curran, M. A. J., van Ommen, T. D., Morgan, V. I., Phillips, K. L., & Palmer, A. S. (2003). Ice core evidence for Antarctic sea ice decline since the 1950s. *Science*, *302*(5648), 1203–1206. https://doi.org/10.1126/science.1087888

Dalaiden, Q., Goosse, H., Rezsohazy, J., & Thomas, E. R. (2021). Reconstructing atmospheric circulation and sea-ice extent in the West Antarctic over the past 200 years using data assimilation. *Climate Dynamics*, *57*(11–12), 3479–3503. https://doi.org/10.1007/s00382-021-05879-6

Eayrs, C., Holland, D., Francis, D., Wagner, T., Kumar, R., & Li, X. C. (2019). Understanding the seasonal cycle of Antarctic sea ice extent in the context of longer-term variability. *Reviews of Geophysics*, *57*(3), 1037–1064. https://doi.org/10.1029/2018rg000631

Fetterer, F., Knowles, K., Meier, W. N., Savoie, M., & Windnagel, A. K. (2017). Sea Ice Index, Version 3. Average daily sea ice extend and area, using 5-day trailing averages. In N. N. S. a. I. D. Center (Ed.), *Square kilometers, by region of the Antarctic ocean. Ancillary analysis spreadsheets*.

Fogt, R. L., & Bromwich, D. H. (2006). Decadal variability of the ENSO teleconnection to the high latitude South Pacific governed by coupling with the southern annular mode. *Journal of Climate*, *19*(6), 979–997. https://doi.org/10.1175/jcli3671.1

Fogt, R. L., Jones, J. M., & Renwick, J. (2012). Seasonal zonal asymmetries in the southern annular mode and their impact on regional temperature anomalies. *Journal of Climate*, *25*(18), 6253–6270. https://doi.org/10.1175/jcli-d-11-00474.1

Fogt, R. L., Sleinkofer, A. K., Raphael, M. N., & Handcock, M. S. (2022). A regime shift in seasonal total Antarctic sea ice extent in the twentieth century. *Nature Climate Change*, *12*(1), 54–62. https://doi.org/10.1038/s41558-021-01254-9

Hersbach, H., Bell, B., Berrisford, P., Biavati, G., Horányi, A., Muñoz Sabater, J., et al. (2018). ERA5 hourly data on single levels from 1979 to present. *Copernicus Climate Change Service (C3S) Climate Data Store (CDS)*, *10*. https://doi.org/10.24381/cds.adbb2d47

Hersbach, H., Bell, B., Berrisford, P., Hirahara, S., Horanyi, A., Munoz-Sabater, J., et al. (2020). The ERA5 global reanalysis. *Quarterly Journal of the Royal Meteorological Society*, *146*(730), 1999–2049. https://doi.org/10.1002/qj.3803

Holland, M. M., Landrum, L., Raphael, M., & Stammerjohn, S. (2017). Springtime winds drive Ross Sea ice variability and change in the following autumn. *Nature Communications*, *8*(1), 731. https://doi.org/10.1038/s41467-017-00820-0

HoHolland, M. M., Landrum, L., Raphael, M. N., & Kwok, R. (2018). The regional, seasonal, and lagged influence of the Amundsen Sea Low on Antarctic sea ice. *Geophysical Research Letters*, *45*(20), 11227–11234. https://doi.org/10.1029/2018gl080140

Jena, B., Bajish, C. C., Turner, J., Ravichandran, M., Kshitija, S., Kumar, A. N., et al. (2022). *Mechanisms associated with the rapid decline in sea ice cover around a stranded ship in the Lazarev Sea, Antarctica*. Science of the Total Environment. https://doi.org/10.1016/j.scitotenv.2022.153379

Jena, B., Bajish, C. C., Turner, J., Ravichandran, M., Kumar, A. N., & Kshitija, S. (2022). Record low sea ice extent in the Weddell Sea, Antarctica in April/May 2019 driven by explosive polar cyclones. *Climate and Atmospheric Science*, *5*(1), 19. https://doi.org/10.1038/s41612-022-00243-9

Kohout, A. L., Williams, M. J. M., Dean, S. M., & Meylan, M. H. (2014). Storm-induced sea-ice breakup and the implications for ice extent. *Nature*, *509*(7502), 604–607. https://doi.org/10.1038/nature13262

Lefebvre, W., Goosse, H., Timmermann, R., & Fichefet, T. (2004). Influence of the southern annular mode on the sea ice-ocean system. *Journal of Geophysical Research*, *109*(C9), C09005. https://doi.org/10.1029/2004JC002403

Li, X., Cai, W., Meehl, G. A., Chen, D., Yuan, X., Raphael, M., et al. (2021). Tropical teleconnection impacts on Antarctic climate changes. *Nature Reviews Earth & Environment*, *2*(10), 680–698. https://doi.org/10.1038/s43017-021-00204-5

Meehl, G. A., Arblaster, J. M., Bitz, C. M., Chung, C. T. Y., & Teng, H. Y. (2016). Antarctic sea-ice expansion between 2000 and 2014 driven by tropical Pacific decadal climate variability. *Nature Geoscience*, *9*(8), 590–595. https://doi.org/10.1038/ngeo2751

Meier, W. N., Stewart, J. S., Wilcox, H., Hardman, M. A., & Scott, D. J. (2021). *Near-real-time DMSP SSMIS daily polar gridded sea ice concentrations*. Version 2. NASA National Snow and Ice Data Center Distributed Active Archive Center. https://doi.org/10.5067/YTTHO2FJQ97K

Raphael, M. N., & Hobbs, W. (2014). The influence of the large-scale atmospheric circulation on Antarctic sea ice during ice advance and retreat seasons. *Geophysical Research Letters*, *41*(14), 5037–5045. https://doi.org/10.1002/2014gl060365

Raphael, M. N., Marshall, G. J., Turner, J., Fogt, R. L., Schneider, D. P., Dixon, D. A., et al. (2015). *The Amundsen Sea low: Variability, change and impact on antarctic climate* (pp. 111–121). Bulletin of the American Meteorological Society. https://doi.org/10.1175/BAMS-D-14-00018.1

Stammerjohn, S., Martinson, D. G., Smith, R. C., Yuan, X., & Rind, D. (2008). Trends in Antarctic annual sea ice retreat and advance and their relation to El Niño-Southern Oscillation and Southern Annular Mode variability. *Journal of Geophysical Research*, *113*(C3), C03S90. https://doi.org/10.1029/2007JC004269

Thomas, E. R., & Abram, N. J. (2016). Ice core reconstruction of sea ice change in the Amundsen-Ross Seas since 1702 *AD*. *Geophysical Research Letters*, *43*(10), 5309–5317. https://doi.org/10.1002/2016gl068130

Thomas, E. R., Allen, C. S., Etourneau, J., King, A. C. F., Severi, M., Winton, V. H. L., et al. (2019). Antarctic sea ice proxies from marine and ice core archives suitable for reconstructing sea ice over the past 2000 years. *Geosciences*, *9*(12), 506. https://doi.org/10.3390/geosciences9120506

Turner, J. (2004). The El Niño-Southern Oscillation and Antarctica. *International Journal of Climatology*, *24*, 1–31. https://doi.org/10.1002/joc.965

Turner, J., Hosking, J. S., Bracegirdle, T. J., Marshall, G. J., & Phillips, T. (2015). *Recent changes in Antarctic sea ice*. Philosophical Transactions of the Royal Society of London, Series A. https://doi.org/10.1098/rsta.2014.0163

Turner, J., Phillips, T., Hosking, S., Marshall, G. J., & Orr, A. (2013). The amundsen sea low. *International Journal of Climatology*, *33*(7), 1818–1829. https://doi.org/10.1002/joc.3558

Vernet, M., Geibert, W., Hoppema, M., Brown, P. J., Haas, C., Hellmer, H. H., et al. (2019). The Weddell Gyre, Southern Ocean: Present Knowledge and future challenges. *Reviews of Geophysics*, *57*(3), 623–708. https://doi.org/10.1029/2018rg000604

Vichi, M., Eayrs, C., Alberello, A., Bekker, A., Bennetts, L., Holland, D., et al. (2019). Effects of an explosive polar cyclone crossing the Antarctic marginal ice zone. *Geophysical Research Letters*, *46*(11), 5948–5958. https://doi.org/10.1029/2019gl082457

Yang, J., Xiao, C. D., Liu, J. P., Li, S. T., & Qin, D. H. (2021). Variability of Antarctic sea ice extent over the past 200 years. *Science Bulletin*, *66*(23), 2394–2404. https://doi.org/10.1016/j.scib.2021.07.028

References From the Supporting Information

Kaufman, D. E., Friedrichs, M. A. M., Smith, W. O., Queste, B. Y., & Heywood, K. J. (2014). Biogeo-chemical variability in the southern Ross Sea as observed by a glider deployment. *Deep-Sea Research Part I Oceanographic Research Paper*, *92*, 93–106. https://doi.org/10.1016/j.dsr.2014.06.011